AIAA Journal
Vol. 46, No. 9, September 2008

Efficient Implementation of Tam and Auriault's Time-Domain Impedance Boundary Condition

Yves Reymen,* Martine Baelmans,† and Wim Desmet‡
Katholieke Universiteit Leuven, B-3001 Leuven, Belgium

DOI: 10.2514/1.35876

A new and efficient time-domain implementation is proposed for the impedance model originally introduced by Tam and Auriault (Tam, C. K. W., and Auriault, L., "Time-Domain Impedance Boundary Conditions for Computational Aeroacoustics," *AIAA Journal*, Vol. 34, No. 5, May 1996, pp. 917–923). In the frequency domain, the pressure can be calculated from the product of the impedance with the normal velocity. In the time domain, a convolution is needed, which may become a costly operation. Present solutions for this problem involve either a full convolution and storage of a time history of data or a translation of the frequency-domain models to time-domain formulations involving time derivatives. The former approach is very costly in terms of memory and CPU time; the latter makes the implementation discretization specific and vulnerable to stability issues. A new formulation, based on recursive convolution, results in an efficient implementation that stores only one accumulator, which can be updated at each time step with minimal addition and multiplication. It allows for the exact representation of the impedance at a given frequency. The formulation is validated by a comparison with the measurement data from the NASA Langley Grazing Flow Impedance Tube. The simulations are performed by introducing a plane wave at a single frequency in the tube, and this is done for six frequencies and five different mean flow speeds.

I. Introduction

In many aeroacoustic applications, lining material plays an important role in controlling the emitted noise levels. To be able to study the effect of different materials and to judge their effectiveness, adequate numerical models are essential. Optimization of the noise reduction becomes possible by numerical sensitivity analyses of the various material parameters and the geometrical layout.

Most often, lining material is acoustically characterized in the frequency domain. This is usually done by setting up a test with a single harmonic wave excitation and identifying the impedance from the forced response. The obtained complex value is the impedance at the frequency of the harmonic wave excitation. This procedure can only describe linear effects.

Time-domain computational methods have a clear advantage over frequency-domain methods not only for broadband problems, nonlinear interaction investigations, and transient wave simulations, but also for large problems (e.g., three-dimensional high frequencies) [1,2]. To be able to represent an impedance boundary in the time domain, there is a need to "translate" the frequency data to the time domain.

At a given frequency ω, the pressure $P(x_b,\omega)$ in the frequency domain for a position x_b on the lining material is proportional to the normal velocity $V(x_b,\omega)$ by the impedance $Z(\omega)$. A capital indicates the Fourier transform of a quantity. The equivalent expression in the time domain involves the convolution of the inverse Fourier transform, $z(t)$, of the impedance with the velocity [3]. Similar expressions can be given for the admittance $A(\omega)$, which is the inverse of the impedance:

$$\begin{aligned} P(x_b,\omega) &= Z(\omega)\cdot V(x_b,\omega) \\ p(x_b,t) &= z(t)*v(x_b,t) = \int_{-\infty}^{\infty} z(\tau)\cdot v(x_b,t-\tau)\,\mathrm{d}\tau \end{aligned} \tag{1}$$

$$\begin{aligned} V(x_b,\omega) &= A(\omega)\cdot P(x_b,\omega) \\ v(x_b,t) &= a(t)*p(x_b,t) = \int_{-\infty}^{\infty} a(\tau)\cdot p(x_b,t-\tau)\,\mathrm{d}\tau \end{aligned} \tag{2}$$

To be able to take the inverse Fourier transform of the impedance, Eq. (3), Z has to be known over the entire frequency range. This extension to all possible frequencies poses an initial difficulty and establishes the need for an impedance model. Then the convolution has to be performed, which, in its full form, is a very costly operation (in terms of CPU time) and, in addition, requires the entire time history of the velocity. Similar conclusions hold for the admittance, but with the time history of pressure.

$$z(t) = \int_{-\infty}^{\infty} Z(\omega)e^{i\omega t}\,\mathrm{d}\omega \qquad a(t) = \int_{-\infty}^{\infty} A(\omega)e^{i\omega t}\,\mathrm{d}\omega \tag{3}$$

For an impedance model to be physically feasible, it has to comply with three necessary conditions as indicated by Rienstra [3]. It has to be causal, real, and passive. These conditions are not trivially satisfied by a general polynomial fit to the frequency data. Fortunately, the aforementioned full convolution can be avoided in many ways. These include, without going into further details, replacing $i\omega$ by $\frac{\mathrm{d}}{\mathrm{d}t}$, the z transform, and recursive convolution.

Tam and Auriault [4] proposed a three-parameter model, resembling a mass-spring-damper system, and replaced $i\omega$ by $\frac{\mathrm{d}}{\mathrm{d}t}$. This leads to a formulation with low computational cost, but it is not applicable as a general broadband model because of the limited freedom to make a fit. Ozyoruk et al. [5] proposed a broadband impedance model based on a rational polynomial fit in combination with the z transform. This model is rather sensitive to instabilities, but can be used as a general broadband model. Rienstra [3] proposed a model based on a Helmholtz resonator and the z transform that satisfies all conditions and can be exactly tuned to the impedance at a design frequency using five parameters. The implementation of the extended Helmholtz-resonator model (EHR) [6] requires the storage of a long time history. Fung and Ju [7] proposed a model for the

Presented as Paper 2685 at the 12th AIAA/CEAS Aeroacoustics Conference (27th AIAA Aeroacoustics Conference), Cambridge, Massachusetts, 8–10 May 2006; received 27 November 2007; revision received 19 March 2008; accepted for publication 25 March 2008.

*Ph.D. Student, Department of Mechanical Engineering, Celestijnenlaan 300; yves.reymen@mech.kuleuven.be. Student Member AIAA.

†Professor, Department of Mechanical Engineering, Celestijnenlaan 300; martine.baelmans@mech.kuleuven.be.

‡Professor, Department of Mechanical Engineering, Celestijnenlaan 300; wim.desmet@mech.kuleuven.be.

reflection coefficient, relating incoming and outgoing velocities. This enables the application of a space–time continuation that allows for a noncausal model. The convolution is dealt with by recursion, an idea originally developed in the computational electromagnetics community.

The three-parameter model has found widespread use, in part because of its simplicity. Botteldooren [8] proposed it for room acoustics; Tam and Auriault [4] independently proposed it for aeroacoustics. Zheng and Zhuang proposed a 3-D benchmark for broadband time-domain impedance boundary conditions [9] and used it to validate the formulation of Tam and Auriault. They also applied it to an analytical test case and the NASA flow impedance tube case [10] with a parabolic mean flow profile. Together with Zhuang et al. [11], they analyzed the effect of the boundary-layer thickness of the shear flow profile and found the particle displacement continuity to be the correct boundary condition. Li et al. [12,13] proposed a mean flow correction to the formulation of Tam and Auriault. The extended formulation scales the impedance by a factor that is a function of the mean flow. They called this formulation the effective flow impedance (EFI). Richter et al. [14,15] compared the EHR and EFI and studied the stability of their implementation. Lim et al. [16] applied the formulation of Tam and Auriault to the computation of noise reduction by barriers.

A new efficient formulation for time-domain impedance based on the three-parameter model and recursive convolution [17,18] was proposed by the authors and was applied to an analytical case and the NASA flow impedance tube. The new formulation has also been applied to a turbofan inlet case [19] for the calculation of the attenuation of annular duct modes [20].

The developed formulation can be tuned to any given impedance value at a design frequency and is therefore perfectly suited for single-frequency simulations. The implementation is easy and efficient, as only minimal addition and multiplication are needed at each time step and only one accumulator needs to be stored. There is no need for time derivatives or the storage of a time history of quantities as in existing formulations.

The formulation is incorporated in a quadrature-free discontinuous Galerkin method for the linearized Euler equations [21] and is validated with experimental data from the NASA Langley Grazing Flow Impedance Tube [22]. This is a well-documented benchmark that includes cases with and without mean flow for 26 frequencies. It allows for the testing of the formulation by exciting the tube with a plane wave at a given frequency.

II. Formulation

Although the time domain allows the description of nonlinear effects [23], the models are limited here to linear interactions, as a frequency-domain impedance model is used as starting point.

Looking back to Eq. (1), $z(t)$ can be viewed in terms of linear systems theory as the unit impulse response of the system $Z(\omega)$ [23]. If the system can be described by a rational function in which the polynomial in the numerator has a lower order than that in the denominator, it can be written in the form of a partial fraction expansion with residues A_k and poles p_k, Eq. (4), similar to the model of Fung and Ju for the reflection coefficient [7]:

$$Z(\omega) = \sum_{k=1}^{P} \frac{A_k}{i\omega + p_k} \tag{4}$$

If the order of the numerator is higher than that of the denominator, one can work with the admittance, the inverse of the impedance. The only thing that changes in the formulation is the switch of the position of pressure and velocity. If the order of the numerator and that of the denominator are equal, there is an extra constant term in the model, which is trivial to incorporate.

Here we will focus on the three-parameter model. As will become clear in the next section, we only need two complex poles to represent this model. The complex conjugated poles $\alpha \pm i\beta$ ensure that $a(t)$ is real and determine a second-order system (5). Equation (6) gives the corresponding unit impulse response:

$$A(\omega) = \frac{A_1}{i\omega + p_1} + \frac{A_2}{i\omega + p_2} = \frac{C(i\omega) + D}{(i\omega + \alpha)^2 + \beta^2} \tag{5}$$

$$a(t) = e^{-\alpha t}\left(C\cos(\beta t) + \frac{D - \alpha C}{\beta}\sin(\beta t)\right)H(t) \qquad \alpha \geq 0 \tag{6}$$

The condition $\alpha \geq 0$ is to ensure causality of $a(t)$. $H(t)$ is the Heaviside function.

A. Three-Parameter Impedance Model

For simulations in which only one frequency is excited, it is useful to have a specific model capable of matching any given impedance at that frequency. A suitable frequency-domain model is the three-parameter model, Eq. (7), proposed by Botteldooren [8] and Tam and Auriault [4] and also used by Ju and Fung [24], who called it a damped harmonic oscillator. It can be considered as a mass-spring-damper model; all parameters Z_i have to be positive to fulfill the three fundamental conditions [3]. To be able to apply recursive convolution to this model, it is necessary to work with the admittance A, the inverse of the impedance. The model can then be written in the form of Eq. (5). Equation (9) gives the relation between the parameter sets C, D, α, and β and Z_1, Z_0, and Z_{-1}:

$$Z(\omega) = Z_{-1}/(i\omega) + Z_0 + Z_1(i\omega) = \frac{(i\omega)^2 Z_1 + (i\omega)Z_0 + Z_{-1}}{i\omega} \tag{7}$$

$$A(\omega) = \frac{i\omega}{(i\omega)^2 Z_1 + (i\omega)Z_0 + Z_{-1}} = \frac{C(i\omega) + D}{(i\omega + \alpha)^2 + \beta^2} \tag{8}$$

$$C = 1/Z_1 \qquad D = 0 \qquad \alpha = Z_0/(2Z_1) \qquad \beta = \sqrt{Z_{-1}/Z_1 - \alpha^2} \tag{9}$$

At a design frequency $\bar{\omega}$, the impedance Z is given by the complex number $R + iX$. R is the resistance and X the reactance. Equation (10) gives the link between R and X and Z_1, Z_0, and Z_{-1} from the three-parameter model. The relation between R and Z_0 is straightforward. X has to be somehow distributed over Z_1 and Z_{-1}, while keeping the last two positive for a physically possible model [3]. Here the choice is made to attribute a factor g of the absolute value of the reactance to one of the two Z parameters and a matching value to the other depending on the sign of the reactance; see Eq. (11). The factor g has to be positive to make sure Z_1 and Z_{-1} are positive. An additional condition on g follows from the expression for β: g has to be big enough for β to be real. After some algebra the condition becomes

$$g \geq (-1 + \sqrt{1 + (R/X)^2})/2$$

.

$$Z(\bar{\omega}) = R + iX = Z_0 + i(Z_1\bar{\omega} - Z - 1/\bar{\omega}) \tag{10}$$

$$\begin{aligned} &Z_0 = R, \\ &Z_1 = \frac{(1+g)|X|}{\bar{\omega}} \quad \text{and} \quad Z_{-1} = g|X|\bar{\omega} \quad \text{if } X > 0 \quad \text{or} \\ &Z_1 = \frac{g|X|}{\bar{\omega}} \quad \text{and} \quad Z_{-1} = (1+g)|X|\bar{\omega} \quad \text{if } X < 0 \end{aligned} \tag{11}$$

B. Time-Domain Formulation

The convolution of the admittance impulse response $a(t)$ with the pressure $p(t)$, Eq. (2), can be calculated by recursive convolution thanks to the special form of $a(t)$ and the assumption that the pressure is piecewise constant or piecewise linear within a time step Δt. The derivation is inspired by the work of Luebbers [25] and Kelley and Luebbers [26].

1. Preliminary Considerations

The expression of $a(t)$, Eq. (6), can be simplified by defining the constants K_1 and K_2. Application of Euler's formula for complex numbers allows for a more convenient form:

$$a(t) = e^{-\alpha t}(K_1 \cos(\beta t) + K_2 \sin(\beta t))H(t) \tag{12}$$

$$a(t) = (K_1 \cdot \mathrm{Re}\{e^{(-\alpha+i\beta)t}\} + K_2 \cdot \mathrm{Im}\{e^{(-\alpha+i\beta)t}\})H(t) \tag{13}$$

$\mathrm{Re}\{\cdot\}$ and $\mathrm{Im}\{\cdot\}$ are, respectively, the real and imaginary parts.

The pressure is approximated as piecewise linear within a time step Δt. Assume for the moment that the time step is constant and that the time can be written as $t = n\Delta t$. The pressure at the nth time step is noted as p^n.

$$p(t) = p^n + \frac{p^{n+1} - p^n}{\Delta t}(t - n\Delta t) \quad \text{for } t \in [n\Delta t, (n+1)\Delta t] \tag{14}$$

For the recursive convolution, it is necessary to write that approximation in the reversed time $-\tau$ and shifted by $t = n\Delta t$.

$$p(n\Delta t - \tau) = p^{n-m} + \frac{p^{n-m-1} - p^{n-m}}{\Delta t}(\tau - m\Delta t) \quad \text{for } \tau \in [m\Delta t, (m+1)\Delta t] \tag{15}$$

2. Recursive Convolution

The derivation of the recursive convolution starts from Eq. (2), which gives the normal velocity as the convolution of the impulse response of the admittance with the pressure. The first step is to write that equation in a discrete form and replace the integral over the past time as a sum of integrals over intervals, each the size of one time step. Because of causality, the infinite bounds of the integral are reduced to the interval $[0, t]$.

$$v(n\Delta t) = \int_0^{n\Delta t} a(\tau) \cdot p(n\Delta t - \tau)\,\mathrm{d}\tau = \sum_{m=0}^{n-1} \int_{m\Delta t}^{(m+1)\Delta t} a(\tau) \cdot p(n\Delta t - \tau)\,\mathrm{d}\tau \tag{16}$$

Substitution of the admittance model (13) and the piecewise linear approximation of the pressure (15) in Eq. (16) gives

$$v(n\Delta t) = \sum_{m=0}^{n-1} \int_{m\Delta t}^{(m+1)\Delta t} (K_1 \cdot \mathrm{Re}\{e^{(-\alpha+i\beta)\tau}\} + K_2 \cdot \mathrm{Im}\{e^{(-\alpha+i\beta)\tau}\}) \cdot \left(p^{n-m} + \frac{p^{n-m-1} - p^{n-m}}{\Delta t}(\tau - m\Delta t)\right)\mathrm{d}\tau \tag{17}$$

Using the definitions

$$\hat{\chi}^m = \int_{m\Delta t}^{(m+1)\Delta t} e^{(-\alpha+i\beta)\tau}\,\mathrm{d}\tau \quad \text{and} \quad \hat{\xi}^m = \frac{1}{\Delta t}\int_{m\Delta t}^{(m+1)\Delta t} (\tau - m\Delta t)e^{(-\alpha+i\beta)\tau}\,\mathrm{d}\tau \tag{18}$$

Eq. (17) becomes

$$v(n\Delta t) = K_1 \mathrm{Re}\left\{\sum_{m=0}^{n-1}(p^{n-m}\hat{\chi}^m + (p^{n-m-1} - p^{n-m})\hat{\xi}^m)\right\} \cdots + K_2 \mathrm{Im}\left\{\sum_{m=0}^{n-1}(p^{n-m}\hat{\chi}^m + (p^{n-m-1} - p^{n-m})\hat{\xi}^m)\right\} \tag{19}$$

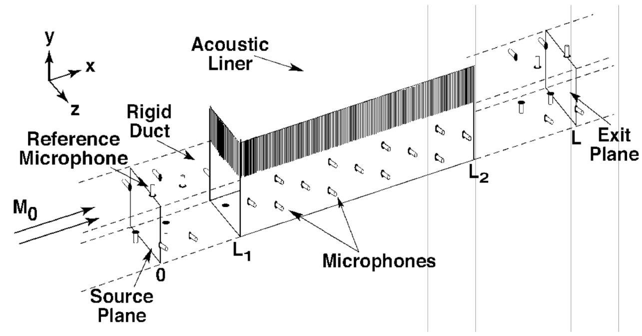

Fig. 1 Measurement setup used for the NASA Langley Grazing Flow Impedance Tube [22].

The complex-valued auxiliary variable $\hat{\psi}$ is defined as the summation over m (the two summations are identical). This variable is an accumulator that can be recursively updated because $\hat{\chi}^{m+1} = e^{(-\alpha+i\beta)\Delta t}\hat{\chi}^m$ and likewise for $\hat{\xi}$. A proof is given in the Appendix.

The resulting formulation of the time-domain impedance using recursive convolution and a piecewise linear approximation of the pressure is given by

$$\hat{\psi}(n\Delta t) = p(n\Delta t)\left(\frac{1 - e^{(-\alpha+i\beta)\Delta t}}{\alpha - i\beta}\right) + (p((n-1)\Delta t) - p(n\Delta t))\left(\frac{e^{(-\alpha+i\beta)\Delta t}((-\alpha+i\beta)\Delta t - 1) + 1}{(-\alpha+i\beta)^2\Delta t}\right) + \hat{\psi}((n-1)\Delta t)e^{(-\alpha+i\beta)\Delta t} \tag{20}$$

$$v(n\Delta t) = K_1 \cdot \mathrm{Re}\{\hat{\psi}(n\Delta t)\} + K_2 \cdot \mathrm{Im}\{\hat{\psi}(n\Delta t)\} \tag{21}$$

If a piecewise constant pressure approximation is used, the update equation for $\hat{\psi}$ is

$$\hat{\psi}(n\Delta t) = p(n\Delta t)\left(\frac{1 - e^{(-\alpha+i\beta)\Delta t}}{\alpha - i\beta}\right) + \hat{\psi}((n-1)\Delta t)e^{(-\alpha+i\beta)\Delta t} \tag{22}$$

As the formulation only depends on the value from the previous time step, the time step may vary. The expression $n\Delta t$ can be replaced again by t. The possibility of working with varying time steps is very useful when working with a Runge–Kutta time stepping scheme, as the length of stages is not equal. Updating of the values can then proceed from one stage to the next without having to extrapolate from previous full time steps [14].

The model obeys all three necessary conditions [3]. Positive α ensures causality. The complex conjugate poles ensure realness. Passivity is guaranteed if the real part of the model is positive. This can be proven by rewriting Eq. (5) in a real part and a imaginary part and by filling in the parameters as described. From this, it follows that the sign of the real part for all frequencies ω is equal to the sign of the resistance R, which is positive for lining materials.

Table 1 Parameters used to model the impedance data at the various frequencies (educed impedance data [22] for case $M = 0$, amplitude 130 dB)

Frequency	g	Z_{-1}	Z_0	Z_1
500	0.5	6068.14	1.0614	2.04944×10^{-4}
1000	5.5	1465.24	0.4903	4.38630×10^{-5}
1500	0.5	5856.09	1.0406	1.97782×10^{-4}
2000	2.5	24240.50	4.1792	2.14907×10^{-4}
2500	0.5	36238.30	1.4986	4.89561×10^{-5}
3000	1.0	11076.00	0.7127	1.55866×10^{-5}

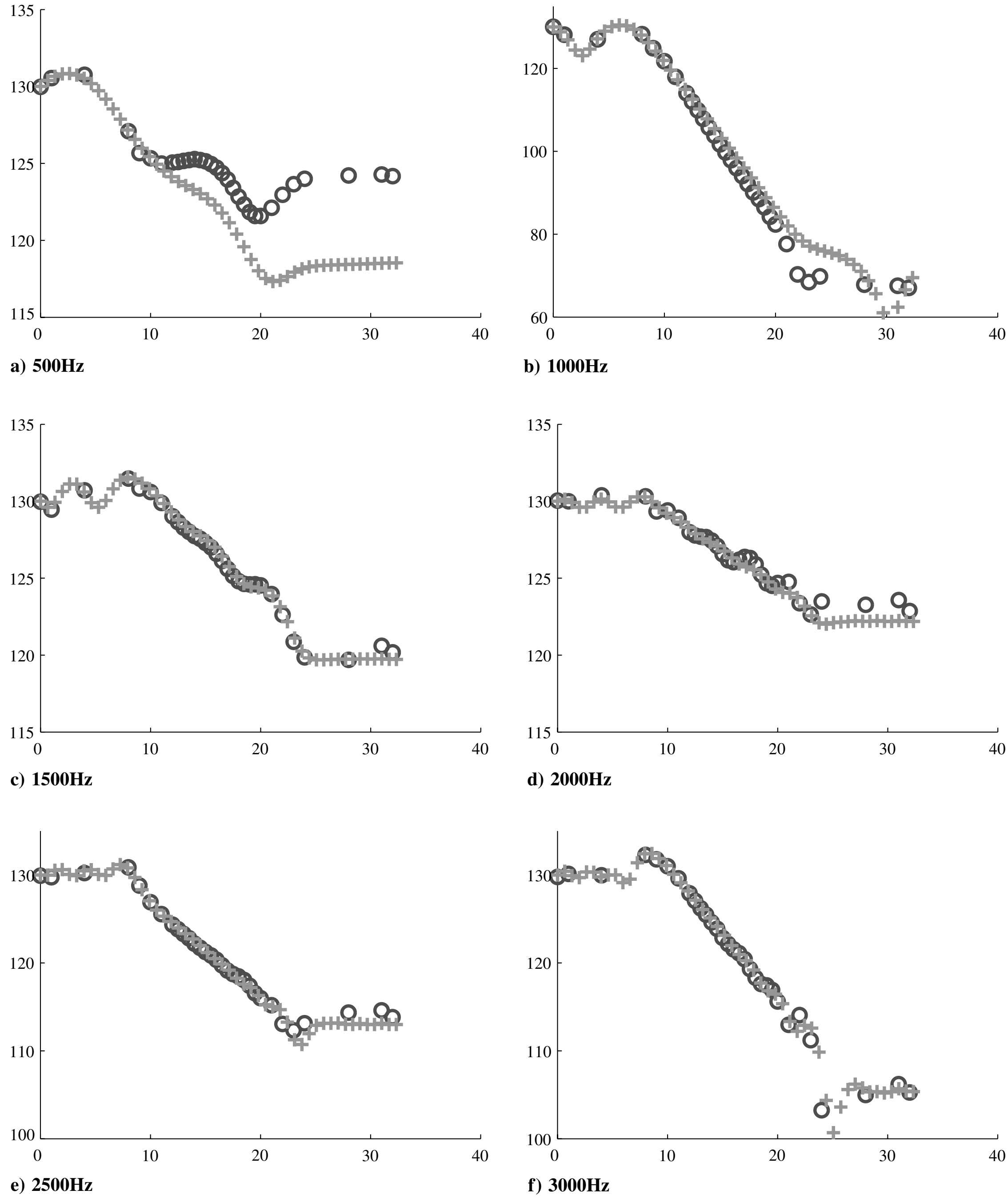

Fig. 2 Sound pressure level (in dB re 2.10^{-5} Pa) along upper wall for Mach 0 as a function of the distance (in inches) along the duct (+: simulation, ○: reference data from measurements).

C. Properties

The formulation exhibits following properties:

Efficiency: The formulation requires minimal addition and multiplication per time step.

Low storage: Storage is needed only for the accumulator in the boundary points. No time history of solution data is required.

Easy implementation: There are no (high-order) time derivatives in the formulation, which allows it to be incorporated in all discretization schemes. Variable time steps are easily accommodated.

Exact single-frequency model: The model is able to represent the exact impedance at a design frequency.

III. Implementation

The admittance formulation is implemented in the framework of a quadrature-free discontinuous Galerkin method for the linearized Euler equations [20,21], supplemented with a low-storage Runge–Kutta time integration [27]. This method allows for the simulation of acoustic propagation through (non)uniform mean flows for 3-D geometries and properly accounts for reflection, refraction, and convection effects.

IV. Results

The NASA Langley Grazing Flow Impedance Tube [22] (see also Fig. 1) is used to characterize different types of liners. In the experiment, plane waves (0.5–3 kHz) are generated at the inlet that propagate through the hard-walled duct. In the middle section, a piece of liner to be tested is installed. The mean flow through the duct can be varied, and tests are performed with Mach numbers ranging from 0 to 0.5 on the centerline.

In the simulation, the inlet section is modeled as a damping zone in which a plane wave with the right frequency is introduced. The hard

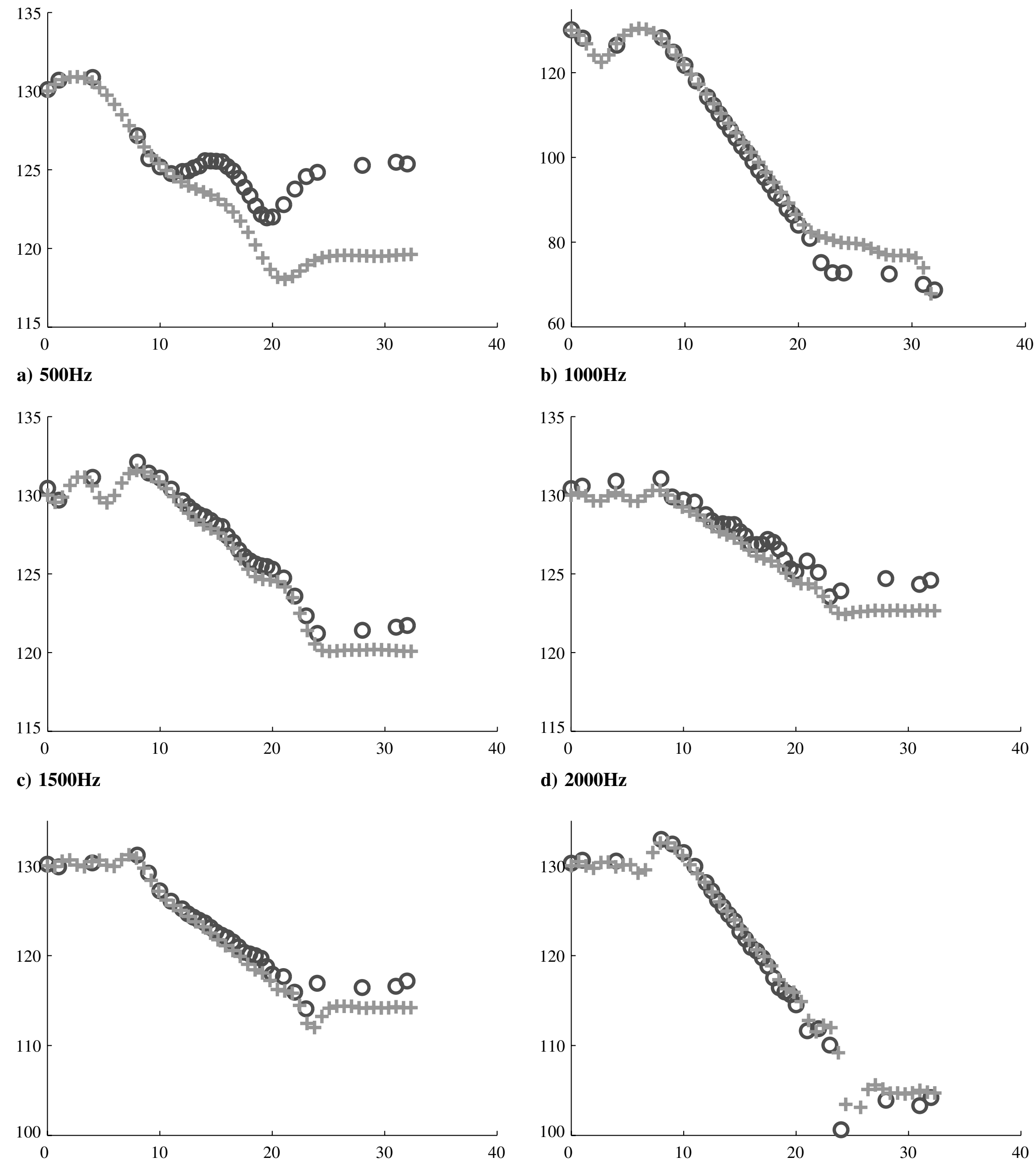

Fig. 3 Sound pressure level (in dB re 2.10^{-5} Pa) along upper wall for Mach 0.1 as a function of the distance (in inches) along the duct (+: simulation, ○: reference data from measurements).

wall is modeled as a perfectly rigid wall with full reflection; the liner is modeled using the proposed time-domain impedance formulation. The outlet section is assumed to be anechoic and is implemented as a damping zone, which ensures low reflections at the outlet.

Table 1 gives for each frequency the value of the parameters used to represent the impedance with the three-parameter model. The factor g, used to distribute the reactance over parameters Z_{-1} and Z_1, is chosen to be just above the limit value of the condition established in Sec. II.A. This is done to produce a slowly oscillating impulse response. The values Z_{-1}, Z_0, and Z_1 are made nondimensional by the characteristic impedance ρc, where $\rho = 1.29\ \mathrm{kg/m^3}$ and $c = 344.283\ \mathrm{m/s}$.

The mean flow is modeled as a parabolic function with the same average mean flow speed as measured. This shear flow approximation seems to be a reasonably good approximation of the real mean flow profile [12,24]. As the mean flow is zero near the wall for a parabolic profile, no correction for the grazing flow needs to be applied to the impedance data.

The domain is discretized with hexahedral elements with size h 1 in. (0.0254 m) in each direction. The duct is 32 in. long and 2 in. high. In the third direction, one element is used and periodic boundary conditions are imposed to simulate in a quasi-two-dimensional way. This is a valid approach as for the studied frequencies only the plane wave mode can propagate. The cut-on frequency is approximately 3.3 kHz for the no-flow case [22]. In the inlet and outlet zone, there are, respectively, 10 and 5 elements in the longitudinal direction. In total, the mesh contains $47 \times 2 \times 1$ elements. The polynomial order p in the discontinuous Galerkin formulation is 2; this gives a spatially third-order accurate method. According to the $(2 * p + 1) \simeq \kappa k h$ rule proposed by Ainsworth [28], with k the wave number and κ a constant equal to about three, this mesh is valid for frequencies up to 3600 Hz.

During each simulation, a time series of pressure data is recorded on the wall opposite of the liner section. This time series is processed with a fast Fourier transform (FFT) to obtain results in the frequency domain. The simulations use a time step of 4×10^{-6} s. The single-

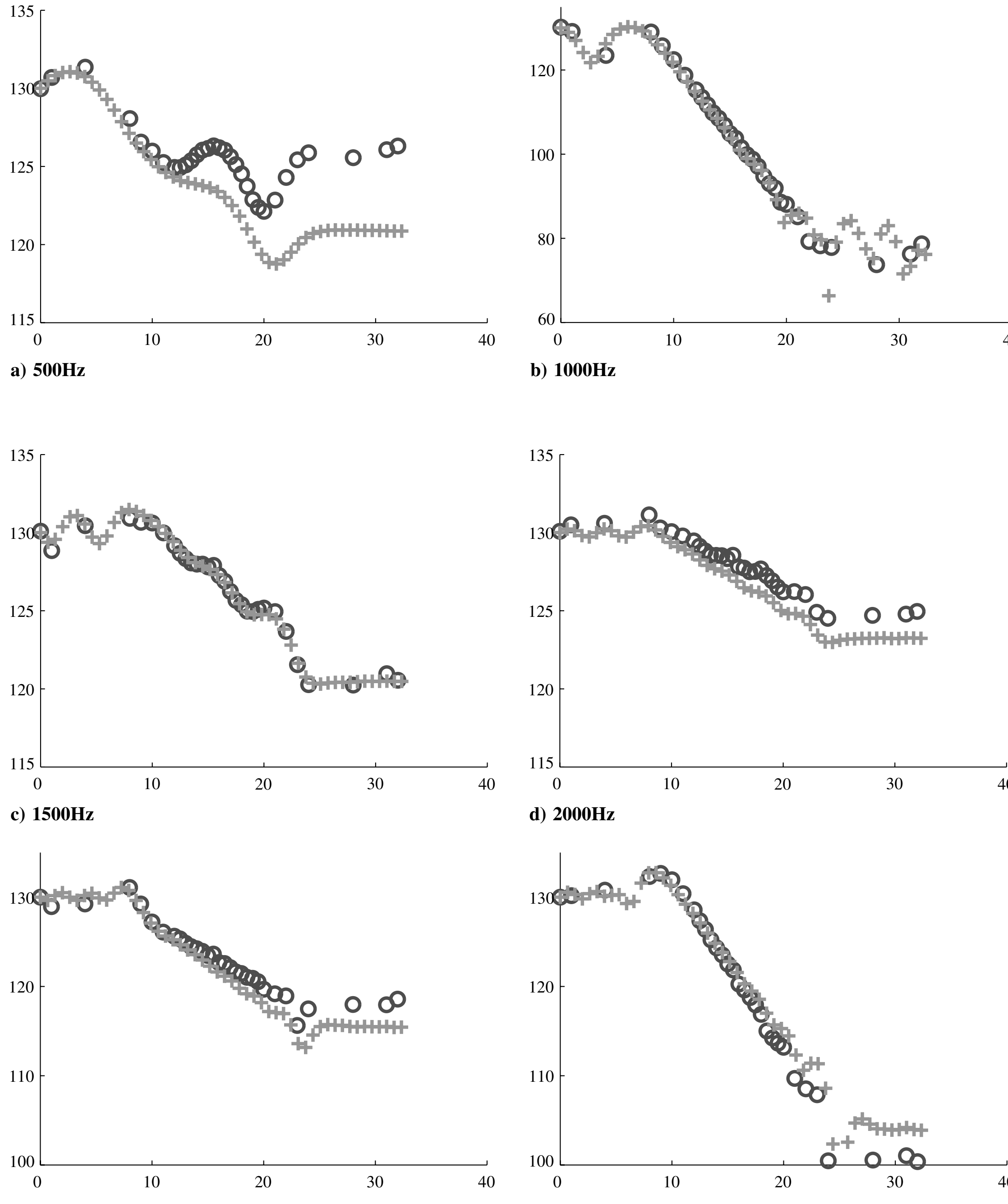

Fig. 4 Sound pressure level (in dB re 2.10^{-5} Pa) along upper wall for Mach 0.2 as a function of the distance (in inches) along the duct (+: simulation, ○: reference data from measurements).

frequency simulations are run from 0 to 0.014 s and the data from the last 0.01 s are used for the FFT.

For all the results shown here, a piecewise linear approximation for the pressure has been used, given the negligible extra cost compared with a piecewise constant approximation. Note that no noticeable difference was seen in the results obtained with the two different choices, probably because of the small time step required by the discretization.

Figure 2 compares the measurement data with the numerical results for the no-flow case. The circles represent the measurements. The plus signs represent the results obtained from a simulation in which one plane wave with that particular frequency is introduced.

For all frequencies except 500 Hz, the results from the simulations correspond very well to the measured data. At 500 Hz, the assumption of anechoic termination in the measurements was questionable and may have corrupted the measurements [22].

Figures 3–6 show the results for the cases with the mean flow ranging from 0.1 to 0.4. Similar conclusions can be drawn as those for the no-flow case: for all frequencies except 500 Hz the agreement is good. The difference between the calculations and the measurements increases as the mean flow speed increases. A more accurate representation of the mean flow, possibly with nonzero velocity at the liner section, could improve the results. The effects associated with a grazing mean flow can be modeled by the formulations of Ingard [29] and Myers [30]. The effective flow impedance scaling [13,14] is a practical formulation for single-frequency calculations based on a limited number of approximations.

V. Conclusions

A new formulation for time-domain impedance based on the three-parameter model that satisfies the three necessary conditions [3] is proposed and validated with the NASA Langley Grazing Flow Impedance Tube case [22] for six frequencies and five different mean flow speeds. It allows for an exact match of the impedance at a design frequency with three parameters. Its implementation is efficient with respect to required CPU time and storage, as it only needs minimal addition and multiplication at each time step and the storage of one accumulator in each boundary point. This is in contrast to existing formulations that often need time derivatives and/or a long time history of data for their implementation. An additional benefit is the possibility of working with varying time steps, which is useful for the variable length stages of a Runge–Kutta time integration scheme. This eliminates the need to extrapolate data from previous time steps, which need to be stored in a buffer.

The single-frequency formulation can be extended with additional terms in the impedance model and, as such, gives sufficient freedom to fit any set of sampled impedance values at multiple frequencies. First results [18] in this direction have been obtained and show the potential of this extension to a broadband time-domain impedance formulation.

Appendix

A proof for the recursive updating starts from the definition of the accumulator and proceeds with the splitting of the term containing the pressure of the last time step. The subsequent algebraic manipulations write the remaining sum as the definition of the accumulator at the previous time step. The most important relationship used is $\hat{\chi}^{m+1} = e^{(-\alpha+i\beta)\Delta t}\hat{\chi}^m$ and likewise for $\hat{\xi}$. This relation follows from the definition in Eq. (18).

$$\psi(n\Delta t) = \sum_{m=0}^{n-1}(p^{n-m}\chi^m + (p^{n-m-1} - p^{n-m})\xi^m) \qquad \text{(A1)}$$

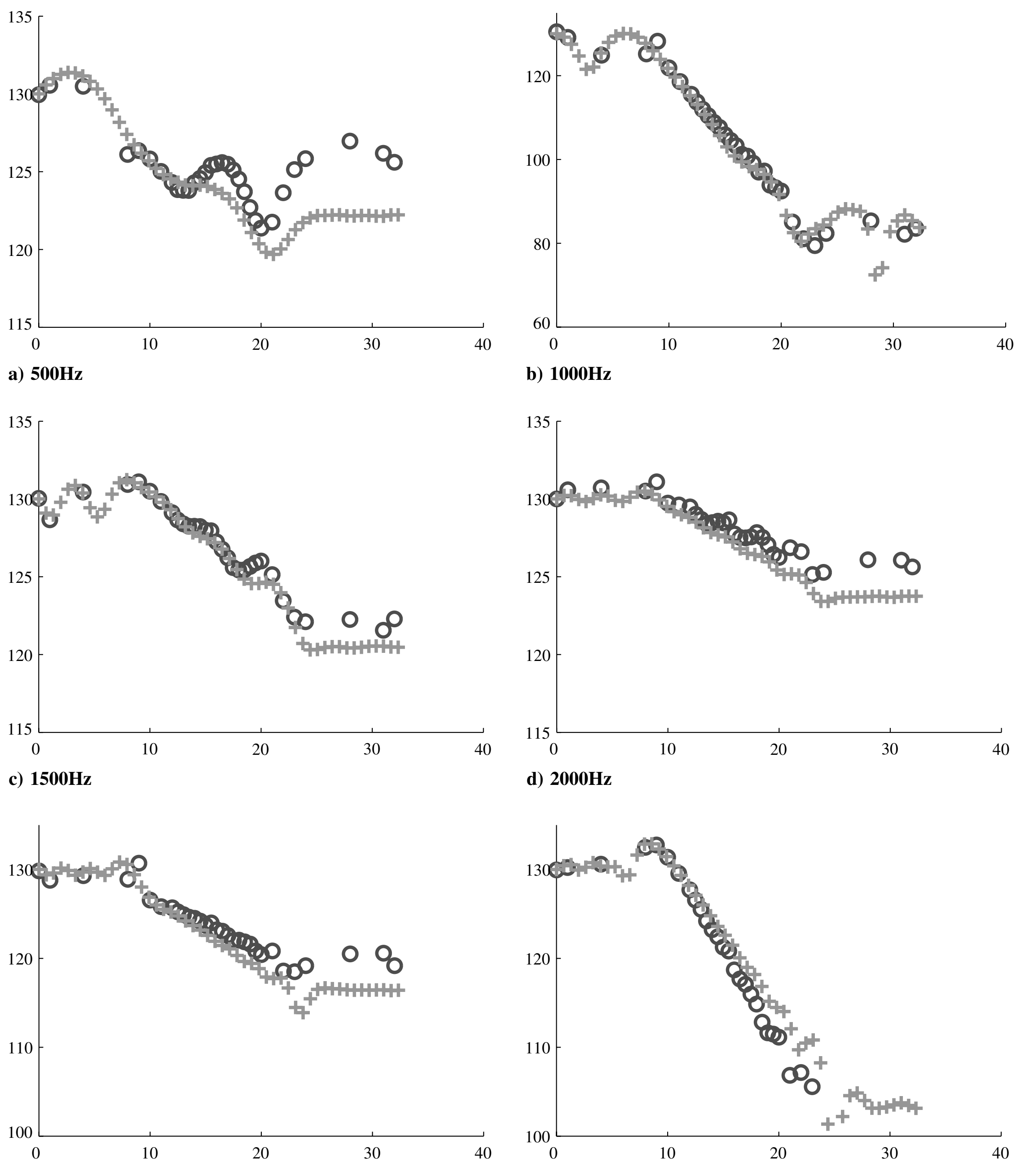

Fig. 5 Sound pressure level (in dB re 2.10^{-5} Pa) along upper wall for Mach 0.3 as a function of the distance (in inches) along the duct (+: simulation, ○: reference data from measurements).

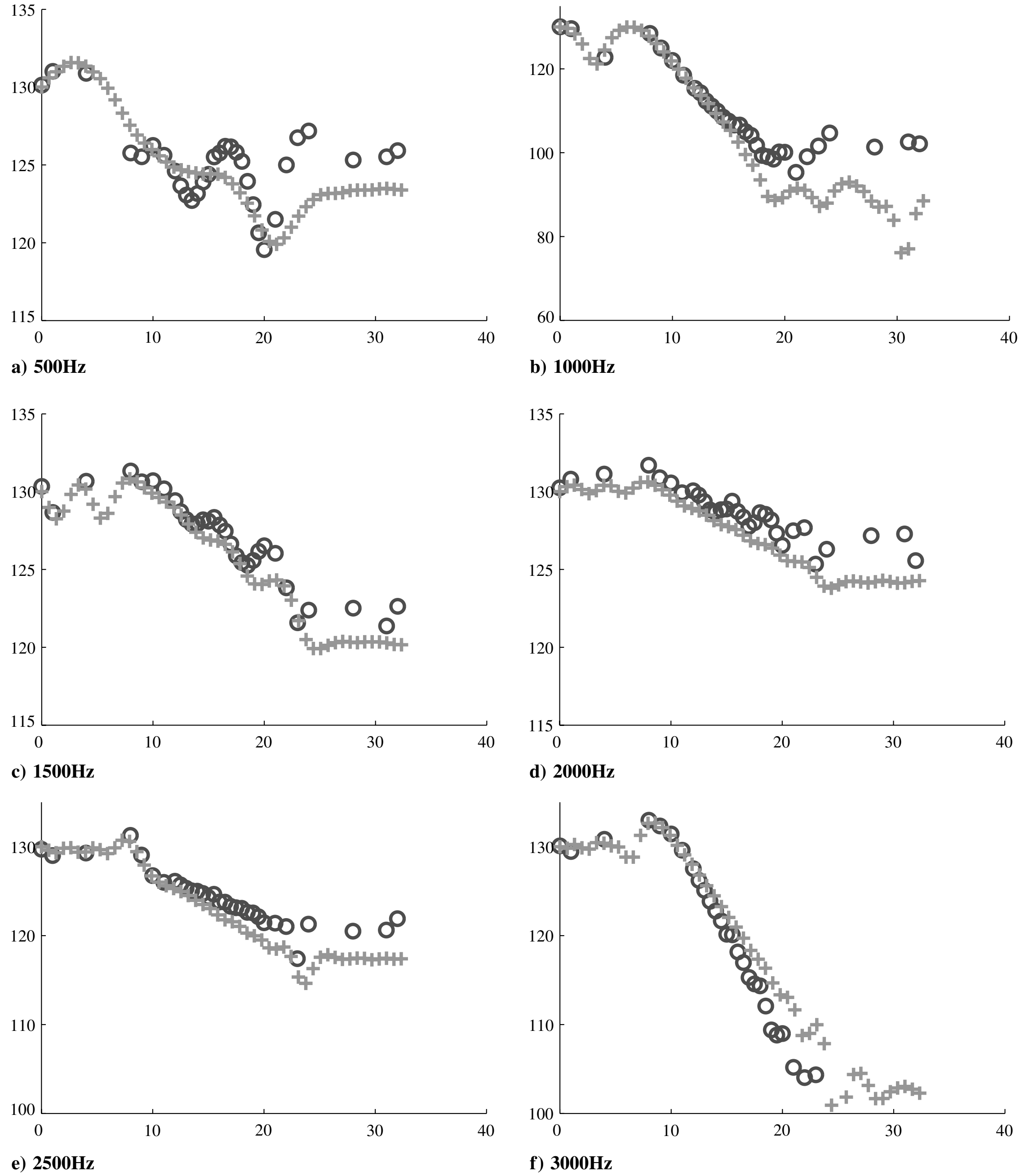

Fig. 6 Sound pressure level (in dB re 2.10^{-5} Pa) along upper wall for Mach 0.4 as a function of the distance (in inches) along the duct (+: simulation, ○: reference data from measurements).

$$= (p^n \chi^0 + (p^{n-1} - p^n)\xi^0) + \sum_{m=1}^{n-1} (p^{n-m}\chi^m + (p^{n-m-1} - p^{n-m})\xi^m) \tag{A2}$$

$$= (p^n \chi^0 + (p^{n-1} - p^n)\xi^0) + \sum_{m=0}^{n-2} (p^{(n-1)-m}\chi^{m+1} + (p^{(n-1)-m-1} - p^{(n-1)-m})\xi^{m+1}) \tag{A3}$$

$$= (p^n \chi^0 + (p^{n-1} - p^n)\xi^0) + e^{(-\alpha+i\beta)\Delta t} \sum_{m=0}^{n-2} (p^{(n-1)-m}\chi^m + (p^{(n-1)-m-1} - p^{(n-1)-m})\xi^m) \tag{A4}$$

$$= (p^n \chi^0 + (p^{n-1} - p^n)\xi^0) + e^{(-\alpha+i\beta)\Delta t}\psi((n-1)\Delta t) \tag{A5}$$

$\hat{\chi}^0$ and $\hat{\xi}^0$ have been replaced in the formulation (20) and (21), through the definition (18), with expressions in terms of the poles $-\alpha + i\beta$ and the time step Δt.

Acknowledgment

The research of Yves Reymen is supported by a fellowship from the Institute for the Promotion of Innovation through Science and Technology in Flanders (IWT-Vlaanderen).

References

[1] Hamilton, J. A., and Astley, R. J., "Acoustic Propagation on Irrotational Mean Flows Using Time-domain Finite and Infinite Elements," AIAA Paper 2003-3280, May 2003.
[2] Chevaugeon, N., Remacle, J.-F., Gallez, X., Ploumhans, P., and Caro, S., "Efficient Discontinuous Galerkin Methods for Solving Acoustic Problems," AIAA Paper 2005-2823, May 2005.
[3] Rienstra, S. W., "Impedance Models in Time Domain Including the Extended Helmholtz Resonator Model," AIAA Paper 2006-2686, May 2006.

[4] Tam, C. K. W., and Auriault, L., "Time-Domain Impedance Boundary Conditions for Computational Aeroacoustics," *AIAA Journal*, Vol. 34, No. 5, May 1996, pp. 917–923.
doi:10.2514/3.13168

[5] Ozyoruk, Y., Long, L. N., and Jones, M. G., "Time-Domain Numerical Simulation of a Flow-Impedance Tube," *Journal of Computational Physics*, Vol. 146, Oct. 1998, pp. 29–57.
doi:10.1006/jcph.1998.5919

[6] Chevaugeon, N., Remacle, J.-F., and Gallez, X., "Discontinuous Galerkin Implementation of the Extended Helmholtz Resonator Model in Time Domain," AIAA Paper 2006-2569, May 2006.

[7] Fung, K.-Y., and Ju, H., "Broadband Time-Domain Impedance Models," *AIAA Journal*, Vol. 39, No. 8, Aug. 2001, pp. 1449–1454.

[8] Botteldooren, D., "Finite-Difference Time-Domain Simulation of Low-Frequency Room Acoustic Problems," *Journal of the Acoustical Society of America*, Vol. 98, No. 6, Dec. 1995, pp. 3302–3308.
doi:10.1121/1.413817

[9] Zheng, S., and Zhuang, M., "Three-Dimensional Benchmark Problem for Broadband Time-Domain Impedance Boundary Conditions," *AIAA Journal*, Vol. 42, No. 2, Feb. 2004, pp. 405–407.
doi:10.2514/1.9102

[10] Zheng, S., and Zhuang, M., "Verification and Validation of Time-Domain Impedance Boundary Conditions in Lined Ducts," *AIAA Journal*, Vol. 43, No. 2, Feb. 2005, pp. 306–313.
doi:10.2514/1.7214

[11] Zhuang, M., Zheng, S., and Thiele, F., "Time-Domain Impedance Boundary Conditions for Slip Mean Flow Boundary," *Proceedings in Applied Mathematics and Mechanics*, Vol. 4, Dec. 2004, pp. 530–531.
doi:10.1002/pamm.200410246

[12] Li, X. D., and Thiele, F., "Numerical Computation of Sound Propagation in Lined Ducts by Time-Domain Impedance Boundary Conditions," AIAA Paper 2004-2902, May 2004.

[13] Li, X. D., Richter, C., and Thiele, F., "Time-Domain Impedance Boundary Conditions for Surfaces with Subsonic Mean Flow," *Journal of the Acoustical Society of America*, Vol. 119, No. 5, May 2006, pp. 2665–2676.
doi:10.1121/1.2191610

[14] Richter, C., Thiele, F., Li, X. D., and Zhuang, M., "Comparison of Time-Domain Impedance Boundary Conditions for Lined Duct Flows," *AIAA Journal*, Vol. 45, No. 6, June 2007, pp. 1333–1345.
doi:10.2514/1.24945

[15] Richter, C., and Thiele, F. H., "The Stability of Time Explicit Impedance Models," AIAA Paper 2007-3538, May 2007.

[16] Lim, C. W., Cheong, C., Shin, S.-R., and Lee, S., "Time-Domain Numerical Computation of Noise Reduction by Diffraction and Finite Impedance of Barriers," *Journal of Sound and Vibration*, Vol. 268, Nov. 2003, pp. 385–401.
doi:10.1016/S0022-460X(02)01534-1

[17] Reymen, Y., Baelmans, M., and Desmet, W., "Time-Domain Impedance Formulation based on Recursive Convolution," AIAA Paper 2006-2685, May 2006.

[18] Reymen, Y., Baelmans, M., and Desmet, W., "Time- Domain Impedance Formulation Suited for Broadband Simulations," AIAA Paper 2007-3519, May 2007.

[19] Rienstra, S. W., and Eversman, W., "A Numerical Comparison Between the Multiple Scales and Finite-Element Solution for Sound Propagation in Lined Flow Ducts," *Journal of Fluid Mechanics*, Vol. 437, June 2001, pp. 367–384.
doi:10.1017/S0022112001004438

[20] Reymen, Y., Baelmans, M., and Desmet, W., "Time-domain Simulation of 3D Lined Ducts with Flow by an Unstructured Discontinuous Galerkin Method," International Institute of Acoustics and Vibration Paper 519, July 2007.

[21] Reymen, Y., De Roeck, W., Rubio, G., Baelmans, M., and Desmet, W., "A 3D Discontinuous Galerkin Method for Aeroacoustic Propagation," International Institute of Acoustics and Vibration Paper 387, July 2005.

[22] Watson, W., "Benchmark Data for Evaluation of Aeroacoustic Propagation Codes with Grazing Flow," AIAA Paper 2005-2853, May 2005.

[23] Keefe, L. R., and Reisenthel, P. H., "Time-Domain Characterization of Acoustic Liner Response from Experimental Data Part 1: Linear Response,"AIAA Paper 2005-3060, May 2005.

[24] Ju, H., and Fung, K.-Y., "Time-Domain Impedance Boundary Conditions with Mean Flow Effects," *AIAA Journal*, Vol. 39, No. 9, Sept. 2001, pp. 1683–1690.

[25] Luebbers, R. J., "FDTD for Nth Order Dispersive Media," *IEEE Transactions on Antennas and Propagation*, Vol. 40, No. 11, Nov. 1992, pp. 1297–1301.
doi:10.1109/8.202707

[26] Kelley, D. F., and Luebbers, R. J., "Piecewise Linear Recursive Convolution for Dispersive Media Using FDTD," *IEEE Transactions on Antennas and Propagation*, Vol. 44, No. 6, June 1996, pp. 792–797.
doi:10.1109/8.509882

[27] Carpenter, M. H., and Kennedy, C. A., "A Fourth-Order 2N-Storage Runge-Kutta Scheme," NASA TM 109112, June 1994.

[28] Ainsworth, M., "Dispersive and Dissipative Behaviour of High Order Discontinuous Galerkin Finite Element Methods," *Journal of Computational Physics*, Vol. 198, July 2004, pp. 106–130.
doi:10.1016/j.jcp.2004.01.004

[29] Ingard, U., "Influence of Fluid Motion Past a Plane Boundary on Sound Reflection, Absorption and Transmission," *Journal of the Acoustical Society of America*, Vol. 31, No. 7, July 1959, pp. 1035–1036.
doi:10.1121/1.1907805

[30] Myers, M. K., "On the Acoustic Boundary Condition in the Presence of Flow," *Journal of Sound and Vibration*, Vol. 71, No. 3, Aug. 1980, pp. 429–434.
doi:10.1016/0022-460X(80)90424-1

Z. Wang
Associate Editor